
ACTIVE LEARNING IN SYMBOLIC REGRESSION WITH PHYSICAL CONSTRAINTS

✉ **Jorge Medina**

Department of Chemical Engineering
University of Rochester
jmedina9@ur.rochester.edu

✉ **Andrew D. White***

Department of Chemical Engineering
University of Rochester
andrew.white@rochester.edu

ABSTRACT

Evolutionary symbolic regression (SR) fits a symbolic equation to data, which gives a concise interpretable model. We explore using SR as a method to propose which data to gather in an active learning setting with physical constraints. SR with active learning proposes which experiments to do next. Active learning is done with query by committee, where the Pareto frontier of equations is the committee. The physical constraints improve proposed equations in very low data settings. These approaches reduce the data required for SR and achieves state of the art results in data required to rediscover known equations.

Keywords Symbolic Regression · Query by Committee · Physical Constraints

1 Introduction

A variety of established methods exist for modeling data, ranging from traditional machine learning techniques (linear regression, ridge regression, polynomial regression) to deep learning approaches (neural networks). However, these methods suffer from constraints and/or interpretability, such as limiting the model to a particular shape (e.g., linear), or being too complex to interpret (black box models). Symbolic Regression (SR) is less constrained and searches through the mathematical space of equations. SR allows for discovering a broader range of functional relationships, including those with nonlinear or intricate interactions between variables. [1].

SR is a machine learning technique to propose equations describing data, aiming to identify optimal functional forms and parameters [1, 2]. As the number of features increases, the search space grows exponentially, leading to various strategies to search in such space through evolutionary algorithms, Bayesian models, sparse models, and neural networks [3–8]. SR has been applied successfully to scientific and engineering problems, demonstrating their potential for uncovering real-world mathematical equations. Weng et al. (2009) utilized SR to propose a model for pipe deterioration, while Baichang et al. (2020) leveraged it to introduce a new descriptor for identifying novel perovskite catalysts. More recently, Li et al. (2023) employed SR to determine electron transfer models of minerals under pressure, among other applications.[1, 9–19].

The complexity of ground-truth equations and the presence of noise in the data can hinder the discovery of equations. This occurs in two phases: discoverable and non-discoverable ground truth [20]. Some ground-truth equations possess such complexity that rediscovering them becomes unattainable, even in the absence of noise[20]. This underlies the necessity of devising methods to manage noise and enhance SR. As the ground-truth equation complexity escalates, SR methods often demand many labeled samples, which can incur high costs or require extensive acquisition time. Active learning strategies, such as Query by Committee (QBC), can tackle these challenges by reducing the number of data needed through the intelligent selection of the most informative samples for labeling [21, 22]. In this paper, we introduce two straightforward approaches to reduce the data needed for SR. (I) By incorporating the QBC strategy into the SR framework, and (II) by including soft constraints based on background knowledge in the discovery of equations.

*Corresponding author

The optimization process may not find equations with physical meaning; any equation that fits the data could be found. Applying strict restrictions to search only for physically meaningful equations could make finding suitable expressions as challenging as the optimization itself [23]. As a result, using a soft constraint can effectively guide the search in the desired direction [23]. This reasoning supports our second approach: implementing soft constraints based on prior knowledge to limit the search space appropriately, allowing for faster convergence and better resilience against noisy settings. Various strategies have been employed to address this, such as constraining equations to maintain unit correctness [24], using physical properties to simplify the problem [5, 25], guiding the search for predefined shapes or forms known to be present in the system or deduced from the dataset [25, 26], or checking correctness after equations are rediscovered [19, 27]. Emgle et al, added auxiliary first and second derivatives to be used for constraint optimization [28] Recently, a soft constrained approach was applied to adsorption equations, revealing that some constraints might not work as expected for genetic algorithms [27].

We employ the Feynman dataset as a benchmark for comparing the data points required to rederive equations. AI Feynman[5], at its publication presented state of the art results and is used commonly for performance comparisons. Our findings indicate that our approach frequently surpasses this method in SR. The rest of this paper explores the principles of the active learning technique used, the incorporation of physical constraints, and presents our findings and analysis. As previously states, genetic algorithms are commonly used for SR and its structure can be easily modified.[23]

Genetic Algorithms (GAs) are computational methods inspired by the principles of natural selection, incorporating processes such as reproduction, mutation, and crossover. They involve a population of candidate solutions, referred to as individuals, which consist of components known as genes. Individuals can be represented using various data structures, such as strings, trees, or stacks. Common terms used in GA literature include parents, children, genes and fitness.[23]

The fitness assigns a score to each individual based on how well they perform in solving the target problem. This score is then used to guide the selection process, allowing fitter individuals to have a higher probability of contributing their genetic material to the next generation, thereby promoting the evolution of increasingly effective solutions over time. [23]

In this study, we focus on a specific application of GAs using binary trees as the data structure for representing candidate solutions. Here, the nodes of the tree represent mathematical operators (e.g., +, -, /, sin, cos), while the leaves correspond to either constants or features. This binary tree representation not only serves as an implementation formalism but also aids in visualization for better understanding and interpretation. See Figure 1. For more details on the workings of genetic algorithms, such as initialization, reproduction, crossover, and mutation, please refer to the Supplementary Information (SI).

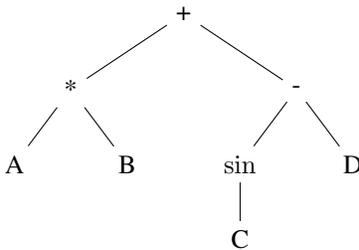


Figure 1: Binary tree representation of the equation $(A * B) + (\sin(C) - D)$

1.1 Inclusion of Background Knowledge: Physical Constraints

In the optimization process, the search is primarily driven by accuracy. However, there is no guarantee that the proposed equation will comply with all the physical constraints of the system, such as divergence, symmetry of variables, or conservation laws. To take advantage of this type of prior knowledge and guide the search towards physically meaningful solutions, the fitness function can be modified to incorporate these constraints as can be seen in Equation 1 where a penalty term is included to balance both accuracy and physical consistency. Given a dataset (\vec{x}, y) of size N and a member of the population ξ the fitness function f is defined as:

$$f(\xi, \vec{x}, y) = L(\xi, \vec{x}, y) + \lambda \phi_k(\xi, \vec{x}) + p_l(\xi) \quad (1)$$

In this equation, $L(\xi, \vec{x}, y)$ represents the Root Mean Square Error (RMSE), quantifying the accuracy of each equation over the dataset. The term ϕ_k serves as a penalty term based on the constraint k , while λ is an adjustable parameter

set to balance the trade-off between accuracy and physical consistency; for our experiments, we've chosen a value of $\lambda = 100$. The complexity of the equations introduces an additional penalty, denoted by p_l , which promotes size homogeneity in the population. Ultimately, the fitness or score of the equation ξ is signified by $f(\xi)$.

Some common types of constraints that can be relevant to chemical engineering applications include divergence, symmetry, and sign constraints. Basically, it 'activates' the penalty when the physical constraint is not complying with the equation.

Divergence is the behavior of a function as its input approaches a particular point. In some cases, it may be necessary to ensure that the function does not diverge (i.e., does not become infinite). For example, in chemical engineering applications, it might be important to guarantee that the concentration of a reactant remains finite. A simple way to represent a divergence constraint is as follows:

$$\phi_{\text{div}}(\xi, a) = \begin{cases} 0, & |\xi(a)| = \infty, \\ 1, & |\xi(a)| \neq \infty. \end{cases} \quad (2)$$

Symmetry, in this context, refers to the property of a function where swapping two variables does not change its value (e.g., $\xi(x_1, x_2) = \xi(x_2, x_1)$) or any example where commutativity applies. This can be particularly relevant in cases where the order of variables should not affect the system's behavior.

$$\phi_{\text{symm}}(\xi, \vec{x}) = \begin{cases} 0, & \xi(x_1, x_2) = \xi(x_2, x_1) \\ 1, & \xi(x_1, x_2) \neq \xi(x_2, x_1) \end{cases} \quad (3)$$

Sign Constraints (Positivity/Negativity) In some systems, measured properties are always positive or negative within a certain domain. For example, this could be relevant when dealing with concentrations, which should always be non-negative. A simple way to represent sign constraints is as follows:

$$\phi_{\text{sign}}(\xi, \vec{x}) = \begin{cases} 0, & \xi(\vec{x}) \geq 0 \\ 1, & \text{otherwise} \end{cases} \quad (4)$$

For negative is the same concept, with the opposite inequality.

Monotonicity Constraints (Increasing/Decreasing Functions) In some systems, the relationship between variables can be strictly increasing or decreasing within a certain domain. For example, this could be relevant when studying the relationship between temperature and pressure in an ideal gas under constant volume, where temperature and pressure are directly proportional. Monotonicity constraints can be represented based on the sign of the derivative as follows:

$$\phi_{\text{mono}}(\xi, \vec{x}_i) = \begin{cases} 0, & \frac{d\xi(\vec{x})}{dx_i} \geq 0 \\ 1, & \text{otherwise} \end{cases} \quad (5)$$

This constraint enforces that the function is either strictly increasing or, flipping the inequality, strictly decreasing (non-positive derivative) within the specified domain or feature.

In addition to these constraints, chemical engineering applications may require the incorporation of other types of physical constraints, such as conservation laws, boundary conditions, or monotonicity constraints, depending on the specific problem being addressed.

1.2 Active Learning

Active learning is a subfield of machine learning that focuses on selecting the most informative samples to label, with the goal of improving the learning performance while minimizing the labeling effort[29–33]. In SR, active learning can be particularly useful for exploring the search space more efficiently and identifying meaningful equations that describe the underlying system. One well-established active learning method is QBC [34–36].

QBC works by selecting a sample based on the disagreement among a group of experts (the committee). Members of this group should be distinct enough that their disagreement provides valuable information, while being consistently good at describing the system being studied. The algorithm can be described as follows:

1. Train a model and select a committee.
2. Estimate labels of an unsampled pool with each member of the committee.

3. Measure and select the label with the highest disagreement.
4. Label the selected point and repeat until necessary.

Disagreement is defined in terms of an unlabeled dataset D_u , and N committee members $K = \{\Xi_1, \Xi_2, \dots, \Xi_N\}$. Each member i makes a prediction on every unlabeled point j , denoted as $\Xi_i(\vec{x}_j) = Y_{ij}$. For this study, committee members are selected from the Pareto frontier, as they represent the models with the best trade-off between accuracy and complexity. They generally provide valuable insights into the whole domain of the system. A depiction of the process can be shown in figure 2

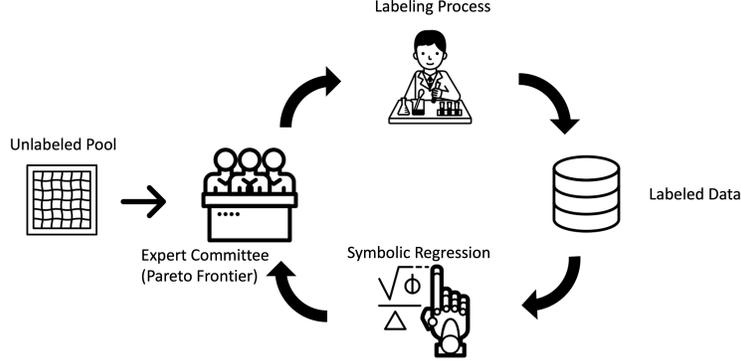


Figure 2: Query By Committee Depiction. Symbolic Regression outputs a Pareto frontier of equations that act as expert models, and measure disagreement from unlabeled data to select the most informative point to label and iterate.

Upon examining the literature, the authors discovered studies that utilized QBC in a SR framework. These studies yielded best results when applied to low complexity equations, where active learning setups were deemed unnecessary since rediscovery occurred with minimal data. However, the approach faced limitations when dealing with high complexity equations.[37]. Bongard et al. [38] discussed the implementation of QBC to generate and sample informative training examples in a grammatical inference problem.

Measurement of Disagreement Measure of disagreements $d(K, \vec{x})$ take the dataset \vec{x} and the committee members K . Two different measures of disagreements were tested. The first measure employed is the coefficient of variation (CV), which is the ratio of the standard deviation (σ) to the mean (μ) of the predicted labels by all members of the committee. This offers a comprehensible metric for assessing the dispersion of the predictions:

$$\mu(K, \vec{x}) = \frac{1}{N} \sum_{i=1}^N \Xi_i(\vec{x}) \quad (6)$$

$$\sigma(K, \vec{x}) = \sqrt{\frac{1}{N} \sum_{i=1}^N (\Xi_i(\vec{x}) - \mu(K, \vec{x}))^2} \quad (7)$$

$$d_{CV}(K, \vec{x}) = \frac{\sigma(K, \vec{x})}{\mu(K, \vec{x})} \quad (8)$$

The coefficient of variation facilitates the comparison of dispersion across different data points or scales.

The second measure is an information-based measure of disagreement [39], which takes into account the relative differences between the predictions:

$$d_{IBMD}(K, \vec{x}) = \frac{1}{|C_2^N|} \sum_{(i,j) \in C_2^N} \log \left(\frac{|\Xi_i(\vec{x}) - \Xi_j(\vec{x})|}{\max(\Xi_i(\vec{x}), \Xi_j(\vec{x}))} + 1 \right) \quad (9)$$

where (ξ_i, ξ_j) represents a pair of equations from the committee, and $|C_2^N|$ is the number of possible pair combinations of N members. The IBMD measure calculates the logarithm of the ratio between the absolute difference of the

predictions and the maximum of the two predictions, incremented by 1. These logarithmic values are then averaged for all possible pair combinations according to Equation 9.

2 Methodology

Our research methodology is structured into three well-defined phases: (I) establishing proof of concept, (II) benchmarking against AI Feynman, and (III) conducting robustness analysis. This design enables a systematic evaluation of our proposed SR approach.

SymbolicRegression.jl or PySR (python front end name) [3] is a Julia package designed for discovering mathematical equations through regularized evolution. This high-performance package offers an efficient implementation of SR, enabling the identification of underlying mathematical relationships within complex data sets. Equation representations are based on binary trees, with numerous hyperparameters for customization. To ensure fair and straightforward comparisons across multiple cases, the same parameters were chosen for all experiments. These primarily consisted of default parameters for the evolutionary process. The maximum number of iterations was adjusted to 100, and the selected binary operators included addition (+), subtraction (−), multiplication (*), and division (/). The chosen unary operators were inverse (inv), square, cube, exponent (exp), square root (*sqrt*), and cosine (cos). Restrictions were applied to prevent nested operators, such as $\cos(\cos(x))$.

The software’s simplicity and efficiency, combined with its ability to customize loss functions, made it a suitable choice for our research. PySR’s use of genetic algorithms leverages Julia’s high-performance computing capabilities, offering a straightforward and adaptable solution for performing SR in our study.

In assessing our methodology, we leveraged the observation that rediscovering an equation often leads to a marked enhancement in accuracy (more than 10 orders of magnitude for noiseless systems), accompanied by a minimal rise in equation complexity (1 or 2). This insight facilitates an automated process for configuring experiments and ascertaining success using loss metrics. Nevertheless, the presence of noise results in a diminished increase in accuracy, making it essential to employ a more hands-on approach for success evaluation, which involves visually examining whether the equation has been successfully rediscovered.

In the initial stage, our primary goal was to demonstrate the effectiveness of our method through a comprehensive toy case focused on the gravitational equation. This aimed to validate the program’s ability to rediscover known equations within a controlled setting. To examine the impact of incorporating physical constraints, we explored the one-dimensional gravity equation: $\frac{Gm_1m_2}{r^2}$. All variables were held constant (number of iterations, operator set, default evolution parameters), with the exception of the fitness function. We acknowledge that, for this equation, given sufficient time (e.g., 100 iterations), the algorithm will inevitably rediscover the equation. Therefore, we limited the number of iterations to 20, making the task more challenging for the algorithm.

Secondly, in order to evaluate the performance of Query By Committee, we set up an active learning scenario involving the following equation: $f = (1/2\pi)^{1/2} \exp(-(x_1 - x_2)/\sigma)^2/2$ from the Feynman dataset. We started with three data points and examined the percentage of rediscovery as new data points were added based on either random sampling, QBC with IBMD, and CV. This stepwise approach allowed us to systematically compare both approaches.

Next, we benchmark the model against AIFeynman, a SR framework using the Feynman equations datasets [5]. This comparison enables us to assess the performance of our approach relative to existing methods, highlighting its strengths and potential weaknesses.

Finally, we subject our model to a series of stress tests, introducing two distinct levels of noise into the data. This stage aims to assess the robustness of our findings when faced with real-world scenarios where data has noise from experiments.

Two notable limitations are that as noise levels increase, fully automated experiments are not possible. Even in cases where the ground truth equation was exactly rediscovered in the Pareto-frontier, there was no big jump in accuracy (around 2 orders of magnitude or less) which could cause false convergence. Consequently, to allow time for human evaluation of success, the experiment was narrowed down to just three representative case examples to assess the model’s performance in the presence of noise. Second, due to the penalty, the loss change was not enough to detect convergence. This presented a challenge in determining the optimal stopping point for the algorithm. To address this issue, it was decided to only use the physical constraints for a limited time during the evolutionary process. After this initial period, the constraints were removed, allowing exploration of a wider range of potential solutions. This approach aimed to strike a balance between guiding the model towards physically meaningful solutions and giving the algorithm freedom to take full advantage of the evolutionary operations with a head start in the right direction. Figure B.3 shows the effectiveness of this approach.

3 Results

3.1 Query By Committee

Both measures of disagreement mentioned earlier appear to function similarly. As depicted in Figure 3a, comparing the disagreement between the equations on the Pareto frontier using either method (CV or IBMD) yielded comparable outcomes. A correlation coefficient close to one was anticipated, since both measurements represent the range of predictions from each equation. Figure 3b demonstrates that employing QBC leads to the more frequent rediscovery of the same equation using fewer data points compared to merely adding new data at random. Consequently, the remaining experiments presented in Figure 4 were conducted using QBC with IBMD.

The findings presented in Figure 4 demonstrate that our model, with the implementation of QBC, outperforms AIFeynman in 8 out of 12 test cases in rediscovering equations using fewer data points. However, it is important to note that AIFeynman’s results were only reported in orders of magnitude of 10 data points, which limited our ability to make a direct comparison between the precise number of data points required for each model.

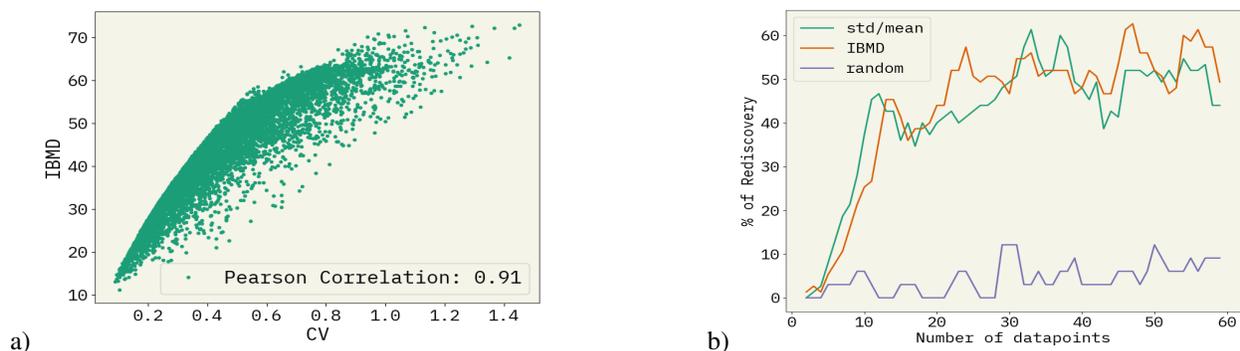


Figure 3: Evaluation of disagreement measures. a) Disagreement analysis of 15 equations from PySR and 10,000 data points, resulting in a correlation coefficient of 0.91. Similar points exhibit maximum disagreement. b) Comparison of $f = (1/2\pi)^{1/2} \exp(-(x_1 - x_2)/\sigma)^2/2$ rediscovery performance versus the number of data points when adding new labeled points through active learning and random addition.

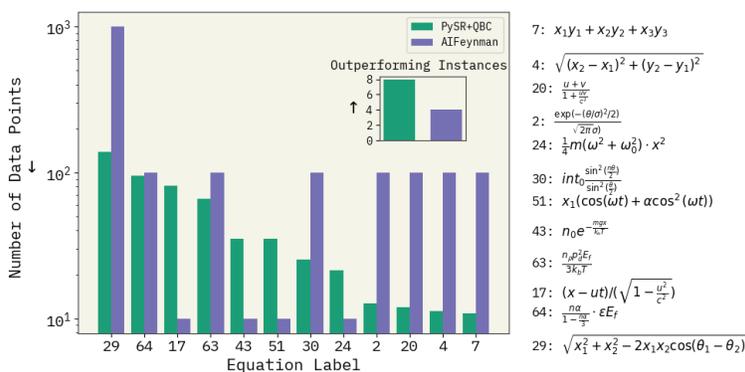


Figure 4: Difference in points needed for rediscovery of non-trivial equations of Feynman dataset. From the twelve tested equations PySR with QBC outperformed in eight of them. Arrows show direction of improvement (lower the better or vice-versa)

3.2 Physical Constraints

To evaluate the effectiveness of incorporating physical constraints and Query By Committee in SR, a proof of concept study was conducted using the well-known gravitational force equation $F = \frac{Gm_1m_2}{r^2}$ as a test case. This equation was chosen due to its simplicity and multiple possible constraints, providing a clear benchmark for assessing the impact of the proposed methods.

Four types of constraints were considered for this experiment: divergence, asymptote, monotonicity, and positivity. The goal was to investigate how each of these constraints affects the ability of SR to rediscover the gravitational force equation.

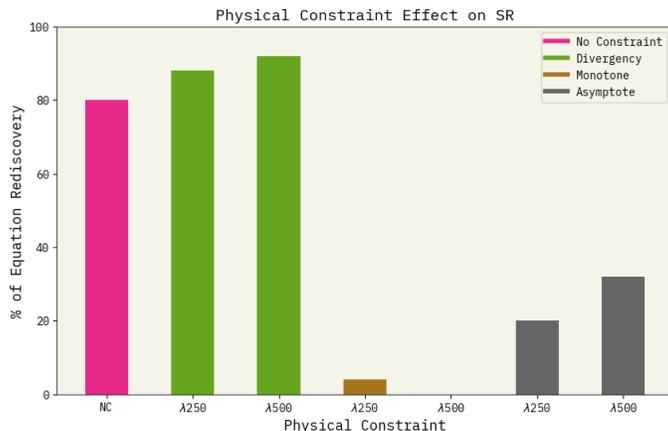


Figure 5: Rediscovery of Gravitational Law with different types of constraints.

Out of the four constraints examined, SR incorporating divergence constraints in the loss function demonstrated superior performance compared to non-constrained regression. This improvement led to an approximately 10% increase in the rediscovery rate, as illustrated in Figure 5. Conversely, the remaining three constraints resulted in reduced performance. Interestingly, even with a relatively simple equation, certain constraints appear to hinder the search in the optimal direction, which may be an indication that even soft constraints can deteriorate the optimization process.

3.3 Robustness Experiments

As previously stated, three distinct equations, selected for their non-triviality and inherent physical constraint, were utilized to assess the method both in noiseless and noisy setups. The noise level was increased to the point where no rediscovery was obtained. In these cases, convergence was rare and not measured enough to obtain valuable statistics. therefore results are either successful (rediscovery) or unsuccessful (No Rediscovery). Table B.2 shows another comparison between un-constrained and constrained optimization where using constraints is able to rediscover the ground truth in a ‘high’ noise level.

The first equation, as depicted in Table 1 and Figure 6, demonstrates an enhancement in rediscovery by employing symmetry constraints, with a p-value of 0.061. Intriguingly and against our expectations, the performance exhibits improvement as noise is added; however, this could be attributed to the inherent limitations of conducting a fully automated process with noise. Owing to false convergence, iterations often converged prematurely, resulting in a higher number of runs with reduced data. Nevertheless, a subtle improvement can be observed in the box plot for both noise experiments.

The other two equations results (SI) show less improvement with constrained optimization. Comparing the complexity of three equations can be seen that for more complex problems constraints have positive effects for optimization.

Table 1: Rediscovery of $\sqrt{x_1^2 + x_2^2} - 2x_1x_2 \cos(\theta_1 - \theta_2)$

Type of Experiment	Noiseless	0.01 Noise	0.1 Noise
No Constraint	213	71.20	No Rediscovery
Symmetry	139	59.19	No Rediscovery

4 Conclusion

This study presents a simple approach to improve Evolutionary Symbolic Regression (ESR) performance by integrating QBC and physical constraints regularization. The proposed method prioritizes informative samples using the Pareto

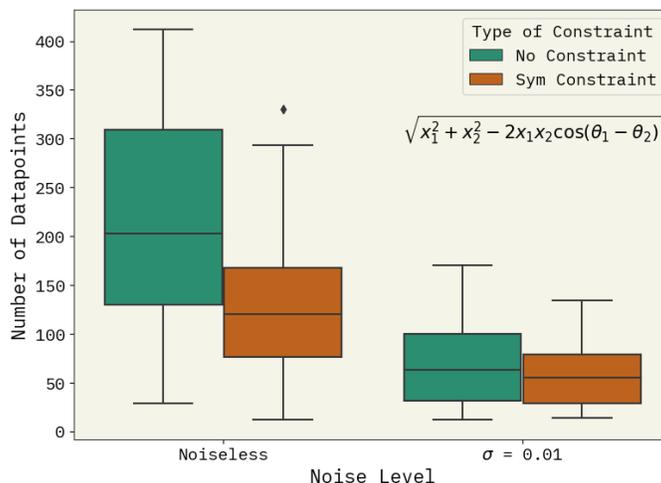


Figure 6: Illustrating the Effects of Noise on Rediscovery: A Comparison between Constrained and Unconstrained Optimizations. The figure presents results for the expression $\sqrt{x_1^2 + x_2^2 - 2x_1x_2\cos(\theta_1 - \theta_2)}$. P-values are 0.061 for noiseless conditions and 0.443 for a noise level of 0.01. The joint p-value for comparing unconstrained and symmetry-constrained optimization is 0.127.

frontier of candidate equations and guides the algorithm toward physically meaningful expressions by incorporating physical constraints as regularization terms.

Our results demonstrate that the application of QBC facilitates the rediscovery of equations using fewer data points than AI Feynman. Moreover, incorporating symmetry as a constraint in symbolic regression showed improvement against a non-constrained regression, while the other constraints, like asymptotes, presented less performance. The removal of constraints needs to be explored more indepth to find the most appropriate level of constraints without hindering the evolutionary process.

The proposed method exhibits resilience against noise, successfully rediscovering equations under various noise levels for specific cases. By integrating QBC and physical constraint regularization, this approach provides a framework for uncovering meaningful mathematical expressions across a wide range of applications, even when faced with limited data.

Acknowledgments

We thank the Center for Integrated Research Computing (CIRC) at the University of Rochester for providing computational resources and technical support.

This work has been supported by funds from the Robert L. and Mary L. Sproull Fellowship gift and U.S. Department of Energy, Grant No. DE-SC0023354.

References

- [1] Michael Schmidt and Hod Lipson. Distilling free-form natural laws from experimental data. *Science*, 324(5923):81–85, 2009.
- [2] JohnR. Koza. Genetic programming as a means for programming computers by natural selection. *Statistics and Computing*, 4(2), June 1994.
- [3] Miles Cranmer. Pysr: Fast & parallelized symbolic regression in python/julia, September 2020.
- [4] Runhai Ouyang, Stefano Curtarolo, Emre Ahmetcik, Matthias Scheffler, and Luca M. Ghiringhelli. SISSO: A compressed-sensing method for identifying the best low-dimensional descriptor in an immensity of offered candidates. *Physical Review Materials*, 2(8):083802, August 2018.
- [5] Silviu-Marian Udrescu and Max Tegmark. AI Feynman: A physics-inspired method for symbolic regression. *Science Advances*, 6(16):eaay2631, April 2020.

- [6] Roger Guimerà, Ignasi Reichardt, Antoni Aguilar-Mogas, Francesco A. Massucci, Manuel Miranda, Jordi Pallarès, and Marta Sales-Pardo. A Bayesian machine scientist to aid in the solution of challenging scientific problems. *Science Advances*, 6(5):eaav6971, January 2020.
- [7] Richa Ramesh Naik, Armi Tiihonen, Janak Thapa, Clio Batali, Zhe Liu, Shijing Sun, and Tonio Buonassisi. Discovering equations that govern experimental materials stability under environmental stress using scientific machine learning. *npj Computational Materials*, 8(1):72, April 2022.
- [8] Martin Schmelzer, Richard P. Dwight, and Paola Cinnella. Discovery of Algebraic Reynolds-Stress Models Using Sparse Symbolic Regression. *Flow, Turbulence and Combustion*, 104(2-3):579–603, March 2020.
- [9] Ben McKay, Mark Willis, and Geoffrey Barton. Steady-state modelling of chemical process systems using genetic programming. *Computers & Chemical Engineering*, 21(9):981–996, 1997.
- [10] William La Cava, Kourosh Danai, and Lee Spector. Inference of compact nonlinear dynamic models by epigenetic local search. *Engineering Applications of Artificial Intelligence*, 55:292–306, 2016.
- [11] E.L. Sanjuán, M.I. Parra, and M.M. Pizarro. Development of models for surface tension of alcohols through symbolic regression. *Journal of Molecular Liquids*, 298:111971, 2020.
- [12] Pascal Neumann, Liwei Cao, Danilo Russo, Vassilios S. Vassiliadis, and Alexei A. Lapkin. A new formulation for symbolic regression to identify physico-chemical laws from experimental data. *Chemical Engineering Journal*, 387:123412, 2020.
- [13] Yanzhang Li, Hongyu Wang, Yan Li, Huan Ye, Yanan Zhang, Rongzhang Yin, Haoning Jia, Bingxu Hou, Changqiu Wang, Hongrui Ding, Xiangzhi Bai, and Anhuai Lu. Electron transfer rules of minerals under pressure informed by machine learning. *Nature Communications*, 14(1):1815, March 2023.
- [14] Weihua Cai, Arturo Pacheco-Vega, Mihir Sen, and K.T. Yang. Heat transfer correlations by symbolic regression. *International Journal of Heat and Mass Transfer*, 49(23):4352–4359, 2006.
- [15] Patrick A. K. Reinbold, Logan M. Kageorge, Michael F. Schatz, and Roman O. Grigoriev. Robust learning from noisy, incomplete, high-dimensional experimental data via physically constrained symbolic regression. *Nature Communications*, 12(1):3219, May 2021.
- [16] Baicheng Weng, Zhilong Song, Rilong Zhu, Qingyu Yan, Qingde Sun, Corey G. Grice, Yanfa Yan, and Wan-Jian Yin. Simple descriptor derived from symbolic regression accelerating the discovery of new perovskite catalysts. *Nature Communications*, 11(1):3513, July 2020.
- [17] Silviu-Marian Udrescu and Max Tegmark. Symbolic progression: Discovering physical laws from distorted video. *Physical Review E*, 103(4):043307, April 2021.
- [18] Luigi Berardi, Zoran Kapelan, Orazio Giustolisi, and Dragan Savic. Development of pipe deterioration models for water distribution systems using epr. 10, 07 2008.
- [19] Arthur Grundner, Tom Beucler, Pierre Gentine, and Veronika Eyring. Data-Driven Equation Discovery of a Cloud Cover Parameterization. 2023.
- [20] Oscar Fajardo-Fontiveros, Ignasi Reichardt, Harry R. De Los Ríos, Jordi Duch, Marta Sales-Pardo, and Roger Guimerà. Fundamental limits to learning closed-form mathematical models from data. *Nature Communications*, 14(1):1043, February 2023.
- [21] Burr Settles. Active learning literature survey. Computer Sciences Technical Report 1648, University of Wisconsin–Madison, 2009.
- [22] H. S. Seung, M. Opper, and H. Sompolinsky. Query by committee. In *Proceedings of the Fifth Annual Workshop on Computational Learning Theory, COLT '92*, page 287–294, New York, NY, USA, 1992. Association for Computing Machinery.
- [23] David E. Goldberg. *Genetic Algorithms in Search, Optimization & Machine Learning*. Addison-Wesley Publishing Company, 1989.
- [24] Wassim Tenachi, Rodrigo Ibata, and Foivos I. Diakogiannis. Deep symbolic regression for physics guided by units constraints: toward the automated discovery of physical laws. 2023.
- [25] Qiang Lu, Jun Ren, and Zhiguang Wang. Using Genetic Programming with Prior Formula Knowledge to Solve Symbolic Regression Problem. *Computational Intelligence and Neuroscience*, 2016:1–17, 2016.
- [26] Arijit Chakraborty, Abhishek Sivaram, and Venkat Venkatasubramanian. Ai-darwin: A first principles-based model discovery engine using machine learning. *Computers & Chemical Engineering*, 154:07470, 2021.
- [27] Charles Fox, Neil Tran, Nikki Nacion, Samiha Sharlin, and Tyler R. Josephson. Incorporating Background Knowledge in Symbolic Regression using a Computer Algebra System. 2023.

- [28] Marissa R. Engle and Nikolaos V. Sahinidis. Deterministic symbolic regression with derivative information: General methodology and application to equations of state. *AIChE Journal*, 68(6), June 2022.
- [29] Rainier Barrett and Andrew D. White. Investigating active learning and meta-learning for iterative peptide design. *Journal of Chemical Information and Modeling*, 61(1):95–105, 2021. PMID: 33350829.
- [30] Natalie S. Eyke, William H. Green, and Klavs F. Jensen. Iterative experimental design based on active machine learning reduces the experimental burden associated with reaction screening. *React. Chem. Eng.*, 5:1963–1972, 2020.
- [31] Burr Settles. Active learning literature survey. Computer Sciences Technical Report 1648, University of Wisconsin–Madison, 2009.
- [32] Yifan Fu, Xingquan Zhu, and Bin Li. A survey on instance selection for active learning. *Knowledge and Information Systems*, 35(2):249–283, May 2013.
- [33] Vu-Linh Nguyen, Mohammad Hossein Shaker, and Eyke Hüllermeier. How to measure uncertainty in uncertainty sampling for active learning. *Machine Learning*, 111(1):89–122, January 2022.
- [34] Nathan Haut, Wolfgang Banzhaf, and Bill Punch. Active learning improves performance on symbolic regression-tasks in stackgp, 2022.
- [35] Yoav Freund, H. Sebastian Seung, Eli Shamir, and Naftali Tishby. Selective Sampling Using Query By Committee. *Machine Learning*, 28(2/3):133–168, 1997.
- [36] Ran Gilad-bachrach, Amir Navot, and Naftali Tishby. Query by committee made real. In Y. Weiss, B. Schölkopf, and J. Platt, editors, *Advances in Neural Information Processing Systems*, volume 18. MIT Press, 2005.
- [37] Nathan Haut, Wolfgang Banzhaf, and Bill Punch. Active Learning Improves Performance on Symbolic RegressionTasks in StackGP. 2022.
- [38] Josh Bongard and Hod Lipson. Active coevolutionary learning of deterministic finite automata. *Journal of Machine Learning Research*, 6(56):1651–1678, 2005.
- [39] Teresa Henriques, Luis Antunes, João Bernardes, Mara Matias, Diogo Sato, and Cristina Costa-Santos. Information-based measure of disagreement for more than two observers: a useful tool to compare the degree of observer disagreement. *BMC Medical Research Methodology*, 13(1):47, December 2013.
- [40] John H. Holland. *Adaptation in Natural and Artificial Systems: An Introductory Analysis with Applications to Biology, Control, and Artificial Intelligence*. The MIT Press, 1992.
- [41] K. A. De Jong. An analysis of the behavior of a class of genetic adaptive systems. 1975.
- [42] Melanie Mitchell. An introduction to genetic algorithms. 1996.

A Supp. Material

A.1 Additional Theory

A.1.1 Initialization, Reproduction, and Crossover in Genetic Algorithms

The more members in the population, the broader the search and the better chance of success, but at the expense of computation time. A random combination of unary and binary operators (e.g., \sin , \cos , $\text{inv}(x)$, $+$, $-$, $*$), variables, and constants are formed to get an initial population. After this, "evolution" can start.

Once the first generation is initialized, reproduction takes place. Reproduction is the process where the 'fittest' members of the population get passed towards the next generation. To decide which member is better, a metric called fitness, considering both accuracy and complexity, is used. The fitness metric can be the Mean Absolute Error or Root Mean Square Error, and complexity is the number of tree nodes. Although it can be customized as needed.

After reproduction, the crossover comes next. Crossover, also known as recombination, is a primary genetic operator in genetic algorithms that generates new offspring solutions by combining the features (genes) of two parents [23, 40]. Inspired by the natural process of sexual reproduction, crossover helps promote genetic diversity and exploration of the search space, which is crucial for solving complex optimization problems [41]. This allows searching outside the original population on the mathematical equation space. This is represented in figure A.1

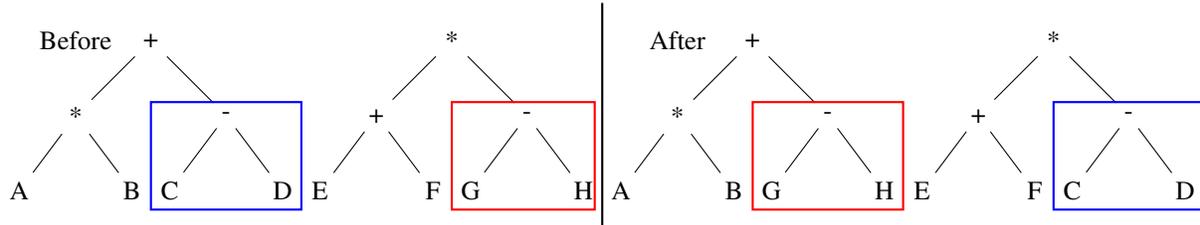


Figure A.1: Crossover depiction between two members of the population

Despite being predominantly heuristic-based, genetic algorithms benefit from the "schema theorem" [23], which formalizes the underlying intuition and provides a theoretical foundation for their effectiveness in optimization and search tasks. Introduced by David E. Goldberg [23], the schema theorem asserts that genetic algorithms inherently operate on multiple schemata concurrently. These schemata, which serve as building blocks or templates, consist of shared characteristics or patterns found in various solutions within the population. According to the schema theorem, the evolutionary process intrinsically rewards advantageous traits (higher fitness) while penalizing undesirable traits (lower fitness) among these schemata. Through iterative selection, crossover, and mutation, genetic algorithms progressively converge towards optimal or near-optimal solutions. Consequently, the schema theorem elucidates the principles behind genetic algorithms, demonstrating their ability to efficiently navigate the search space and identify high-quality solutions to intricate optimization challenges.

A.1.2 Mutation: a safeguard

Mutation is another fundamental genetic operator in genetic algorithms that helps to maintain diversity within the population and prevent premature convergence to suboptimal solutions [23, 42]. It is inspired by the natural process of mutation in biological organisms, where random changes occur in an individual's genetic material. In the context of genetic algorithms, mutation introduces small random alterations to the candidate solutions, or chromosomes, which can lead to the exploration of new points in the search space and thus facilitate the discovery of better solutions.

The mutation step is typically applied after the crossover operation, and its probability is often much lower than that of crossover [41]. There are various mutation operators, and their choice depends on the problem's representation and domain. For example, in a binary-encoded genetic algorithm, a commonly used mutation operator is bit-flip mutation, which involves flipping the value of a randomly selected bit (changing 0 to 1 or vice versa) in a chromosome ([40]).

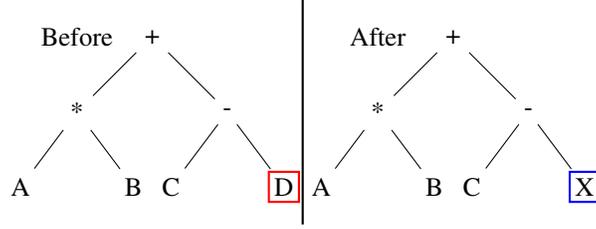


Figure A.2: Mutation depiction of a member of the population

A.2 Inclusion of background knowledge

In the following pseudocode, we present an algorithm that incorporates a penalty term into the loss evaluation process to account for constraint violations. This concise representation demonstrates how to combine the objective function and penalty term using a weight parameter, lambda. By including the penalty term, the algorithm can optimize solutions while adhering to background knowledge and constraints.

Algorithm 1 Inclusion of a Penalty in Loss Evaluation

```

1: procedure EVALUATEWITHPENALTY(population, objectiveFunc, penaltyFunc,  $\lambda$ )
2:   for each individual in population do
3:     loss  $\leftarrow$  objectiveFunc(individual)
4:     penalty  $\leftarrow$  penaltyFunc(individual)
5:     individual.fitness  $\leftarrow$  loss +  $\lambda$  penalty
6:   end for
7: end procedure

```

B Additional Results

We provide evidence of our approach with constraints with the subtree counts on the rediscovery of equation $\frac{1}{\sqrt{(x_2-x_1)^2+(x_4-x_3)^2}}$. As can be seen in the following figure:

We provide tables and plots that illustrate the impact of noise on the rediscovery of equations and the effectiveness of implementing physical constraints. Tables 1 and 2 present the results for the rediscovery of $\frac{1}{2}m(v^2 + u^2 + w^2)$ and $\frac{1}{\sqrt{(x_2-x_1)^2+(y_2-y_1)^2}}$, respectively, under different noise levels and constraint types. Figures 1 and 2 visually represent

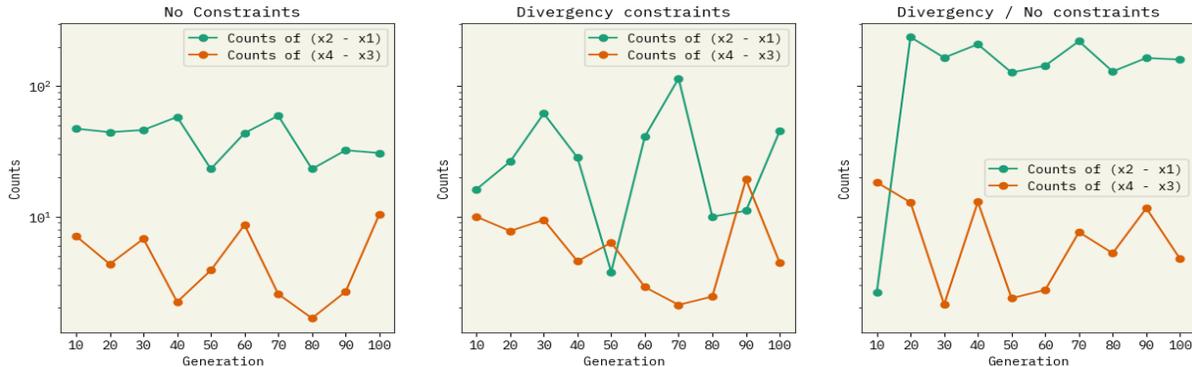


Figure B.3: Counts of substructures $(x_2 - x_1)$ and $(x_4 - x_3)$ for equation $\frac{1}{\sqrt{(x_2-x_1)^2+(x_4-x_3)^2}}$. Results from explorations without rediscovery. It is meant as an indirect measurement if search is performed in the right part of the search space. Without constraints, substructures are very homogeneous but in small amounts. With constraints, substructures seem to appear higher but in a more chaotic way, and a mix of constrained and unconstrained evolution seem to outperformed both methods individually.

these results, providing a clearer comparison between the use of physical constraints and no constraints in the equation rediscovery process.

Table B.1: Rediscovery of $\frac{1}{2}m(v^2 + u^2 + w^2)$

Type of Experiment	Noiseless	0.01 Noise	0.1 Noise
No Constraint	15.61	20.1	18.33
Symmetry	17.4	19.6	21.16

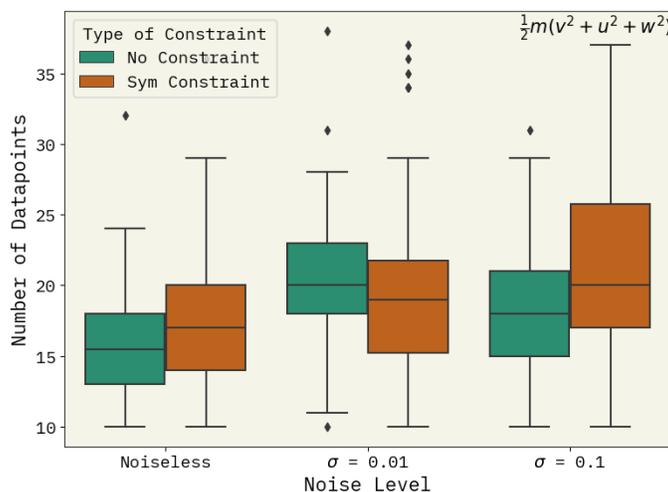


Figure B.4: Illustrating the Effects of Noise on Rediscovery: A Comparison between Constrained and Unconstrained Scenarios. The figure presents results for the expression $\frac{1}{2}m(v^2 + u^2 + w^2)$. P-values are 0.6350 for noiseless conditions, 0.0007 for a noise level of 0.01, and 0.005 for a noise level of 0.1. The joint p-value for comparing unconstrained and constrained optimization under the influence of noise is 0.0002.

The results from the third equation, illustrated in Table B.2 and Figure B.5, do not exhibit any enhancement when compared to unconstrained optimization. In fact, the p-values indicate that a significant difference exists between the constrained and unconstrained methods when no constraints are applied favoring the latter, showing the opposite behaviour. However, when the noise level is increased to 0.1, the ground truth is only rediscovered in the constrained scenario.

Table B.2: Rediscovery of $\frac{1}{\sqrt{(x_2 - x_1)^2 + (y_2 - y_1)^2}}$

Type of Experiment	Noiseless	0.01 Noise	0.1 Noise
No Constraint	11	18	No Rediscovery
Symmetry	16	23	Rediscovery
Divergency	16	23	Rediscovery

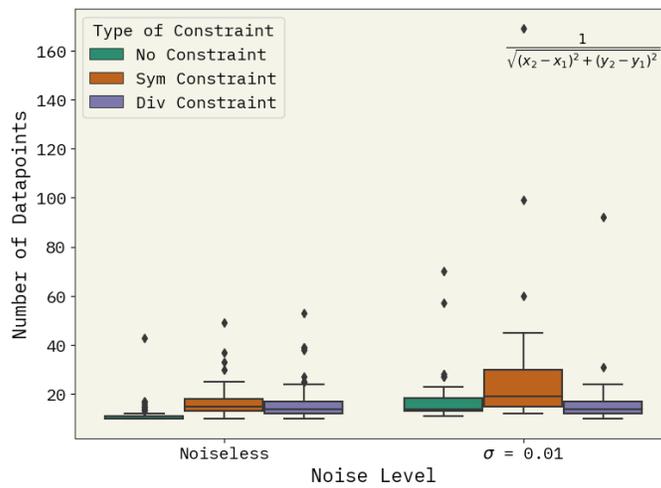


Figure B.5: Illustrating the Effects of Noise on Rediscovery: A Comparison between Constrained and Unconstrained Scenarios. The figure presents results for the expression $\frac{1}{\sqrt{(x_2-x_1)^2+(y_2-y_1)^2}}$. P-values for Symmetry vs No Constraint are 0.0266 for a noise level of 0.01 and 1.22e-11 for noiseless conditions; for Div vs No Constraint, p-values are 0.3319 for a noise level of 0.01 and 3.98e-10 for noiseless conditions. The joint p-value for comparing constrained and unconstrained optimization under the influence of noise is 1.04e-18.